Voltage Profile Improvement in Unbalanced Distribution Grids by Sequential Quadratic Programming

Mohammed Bamatraf
Dept. of Electrical Engineering
Istanbul Technical University
Istanbul, Turkey
matraf21@itu.edu.tr

Oguzhan Ceylan
Dept. of Electrical and Electronic Engineering
Marmara University
Istanbul, Turkey
oguzhan.ceylan@marmara.edu.tr

Ioana Pisica
Dept. of Electrical and Computer Engineering,
Brunel University,
London, UK
ioana.pisica@brunel.ac.uk

Aydogan Ozdemir
Dept. of Electrical Engineering
Istanbul Technical University
Istanbul, Turkey
ozdemiraydo@itu.edu.tr

***Abstract*— The implementation of renewable energy resources (RERs) such as photovoltaic (PV) units and wind turbines (WTs) has been intensively used on active distribution networks (ADNs) due to their significant environmental, technical, and economic benefits. However, their intermittent nature causes some fluctuations in the voltage profiles, which lead to increased losses in the system. This study presents sequential quadratic programming (SQP) optimization method to improve voltage profiles by optimizing tap changer positions and reactive power output of the inverter of a single PV unit. The proposed optimization is applied to the IEEE 34-bus unbalanced distribution test system to validate its performance. Optimum voltage profiles are compared with the base case conditions where there are no PV sources and voltage regulators. The results show that the SQP provides reliable voltage profile improvement for various operational conditions.**

***Index Terms*— Renewable energy resources, active distribution networks, sequential quadratic programming, tap changers, voltage profiles.**

I. Introduction

Renewable energy resources (RERs) such as photovoltaic (PV) systems and wind turbines (WTs) are known for their intermittent nature and unpredictability. One of the main reasons for voltage fluctuations and high losses in distribution networks (DNs) is the lack of sufficient RERs or their inappropriate penetration into the distribution grid. These fluctuations may sometimes result in a violation of the allowable limits [1]. Therefore, the relevant analysis must be performed before integrating renewable energy resources into the DN.

Voltage regulators and capacitor banks have been used for a long time to control the voltage profiles, and the reactive power flows in DNs. However, with the large-scale penetration of the RERs, those traditional regulating devices may not be able to set the voltage profiles, and power flows to their intended values. Moreover, those devices' lifecycle and performance are affected by deterioration due to recurring switching actions [2]. Therefore inverter-interfaced distributed energy resources (DERs) are considered to provide the necessary voltage/VAR control to improve the voltage profile and assure the stability of the DN.

In active distribution networks (ADNs), control-related considerations improve system operations to achieve better efficiency by implementing novel control strategies on the DN to coordinate all DERs integrated into the network and result in better performance [3]. The management and optimization process of ADNs requires solving optimal power flow equations to assure minimum production cost for the distributed generation (DG) units and minimum values for other objective functions [4]. Voltage deviations, active power losses, reliability, and renewable energy hosting capacity are the most popular objective functions. Multi-objective optimization processes are formulated when there are two or more objectives.

Heuristic solution algorithms in [5-7] or the nonlinear programming methods in [8-12] have been proposed to solve such optimization problems. The gradient search and interior point methods have been used to solve the nonlinear programming problem directly. However, such methods require higher computation times. Therefore, faster methods, which involve linearizing the optimization problem, were proposed. The linearized optimization problem, however, may not always converge to the optimal solution and will start to oscillate around non-optimal points [13-17].

This paper focuses on controlling tap changers and reactive power injection from a single PV unit in the unbalanced DN to improve the voltage profiles. At each time step, the model is solved by a proposed Sequential Quadratic Programming Method (SQP) to achieve the best voltage profiles with limited control parameters. The IEEE 34-bus unbalanced feeder is used for implementing the proposed method. The results show that the control actions assure more reliable system operating conditions.

The rest of the paper is organized as follows. In Section II, the problem formulation is given. Section III provides information about the test system and the considered conditions.

TUBITAK and British Council.

2023 IEEE AFRICON | 979-8-3503-3621-4/23/$31.00 ©2023 IEEE | DOI: 10.1109/AFRICON55910.2023.10293298

979-8-3503-3236-0/23/$31.00 ©2023 IEEE

Section IV is devoted to the simulation results. Finally, the paper is concluded on Section V.

II. Problem Formulation

The objective function and constraints of the proposed nonlinear constrained optimization problem are given below.

A. Objective Function (OF)

The main objective of this study is to improve the voltage profiles of the DN. Mathematically, improving the voltage profiles is formulated as minimizing the voltage magnitude deviations from a flat value of 1 pu as expressed in (1).

$$OF = Norm\ [\mathbf{1} - \boldsymbol{V}] \tag{1}$$

where the vector $\boldsymbol{V} = [V_1, V_2, \ldots, V_n]^{\boldsymbol{T}}$ comprises the voltage magnitudes of feeder buses for all phases, and **1** denotes the vector of the same dimension whose all entries are 1. Note that n is 165 for the 34-node system. More details are provided in Sec III, B. The term "Norm" denotes the Euclidean norm of a vector.

B. Equality Constraints (EC)

These constraints refer to the unbalanced power flow equations. The iterative forward-backward sweep method (FBSM) is used in this paper to solve the power flow equations [18]. Equation (2) shows the relationship between the constraints and the control variables;

$$\boldsymbol{V} = PowerFlow\ [\boldsymbol{X}] \tag{2}$$

where $\boldsymbol{X}$ is the control vector, comprising the reactive power output of and transformer tap positions. Assume a part of a radial feeder, as in Fig. 1, whose nodes are enumerated from 1 (starting point) to n (endpoint). For the known voltages of the endpoint bus, all the remaining bus voltages of the feeder can be computed using Kirchhoff's law as in (3)

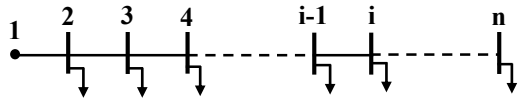

Fig. 1. One phase simple radial system.

$$\dot{V}_{i-1} = \dot{V}_i + \dot{Z}_{i-1,i} * \dot{I}_{i-1,i}\ ;\quad i = 1,2,3,\ldots.,n \tag{3}$$

where $\dot{V}, \dot{I}, \text{and } \dot{Z}$ denote the bus voltage, branch current, and branch impedance phasors, respectively. The subscript *i* and (*i*-1) denote the consecutive bsses along the same phase. The voltage calculations continue up to node-1. This is a direct approach to solve the power flow problem, but it may not converge in radial DN with high R/X ratios. This case can be overcome by using a direct approach. Equation (4) shows the approach used to solve the power flow in radial and weakly meshed networks [19-21];

$$\dot{I}_i = \left[\frac{P_i + jQ_i}{\dot{V}_i}\right]^* \tag{4}$$

Then the relation between the branch currents and equivalent current injections can be found by applying Kirchhoff's current law.

$$\Delta V_i = \text{BCBV} * \text{BIBC} * \dot{\text{I}} \tag{5}$$

$$V_i^{k+1} = V_i^k + \Delta V_i \tag{6}$$

where BCBV is the branch current to bus voltage matrix, and BIBC is the bus injection to branch current matrix. After this step, the backward sweep starts from the starting node until the convergence criteria are satisfied.

C. Inequality Constraints (IC)

Inequality constraints are the limits of bus voltage magnitudes. The feeder bus voltage magnitudes are desired to be between 0.95 and 1.05 pu. A valid formulation for the IC is to check whether the node voltage magnitudes at each time violate the allowable limits as expressed in (7).

$$G_i^j(V_i) = \begin{Bmatrix} 0.95 - V_i & if\ \ V_i < 0.95 \\ 0 & if\ \ 0.95 \le V_i \le 1.05 \\ V_i - 1.05 & V_i > 1.05 \end{Bmatrix} \tag{7}$$

where the subscripts $1 \le i \le 165$ and $1 \le j \le 96$ denote the node number and a 15-minute resolution of a 24 hour simulation time, respectively. A conventional way to deal with IC while optimizing a problem is to express them as a penalty term when the limits are violated. A valid expression is presented in (8).

$$\mathrm{G}^j(\mathbf{V}) = \sum_{i=1}^{165} G_i^j(V_i) \quad j = 1,2,\ldots,96 \tag{8}$$

So, the final formation of the constrained optimization problem for any time (j) is formulated in (9).

$$\begin{matrix} Minimize & OF = \text{Norm}\ [\mathbf{I} - \mathbf{V}] \\ & \boldsymbol{V} = PowerFlow\ [\boldsymbol{X}] \\ Subject\ to & \mathrm{G}^j(\mathbf{V}) \le 0 \end{matrix} \tag{9}$$

D. Control Variables (CV)

There are two types of control variables that are optimized to achieve minimum objective function value.

1. Reactive Power Support of PV Unit (Inverter)

The PV systems are usually equipped with a smart inverter that can provide bi-directional reactive power flow to the feeder in addition to its traditional DC- AC conversion task. Every control parameter is a three-valued vector (one value for each phase) as expressed in (10). Note that the smart inverter supports the reactive power from the PV system only when there is an actual active power generation, in this study, it was assumed so when the generation is over 5% of the rated active power as shown in Fig. 4.

$$Q = [Q_A\ \ Q_B\ \ Q_C]^{\boldsymbol{T}} = [X_1\ \ X_2\ \ X_3]^{\boldsymbol{T}} \tag{10}$$

where the phase reactive powers $Q_A, Q_B, and\ \ Q_C$ are between −120 kVAr and 120 kVAr in this study, which is related to the rating of the PV system and the smart inverter. Note that, depending on the active power generation of the PV panels, reactive power consumption/injection also follows the following power balance equation in (11).

$$Q = \sqrt{S^2 - P^2} \tag{11}$$

2. Tap value of the regulating transformers

There are two regulating transformers (tap changers) allocated between nodes 814-850 and 832-854 in the feeder.

Their tap positions are included in the optimization problem as three-valued vectors as shown in (12). It is worth mentioning that the values of the vector will only take integer numbers between [-16, 16] because they have fixed positions and at every tap action, the voltage level can change by a fixed ratio of 0.00625 pu.

$$T_1 = [X_4\ X_5\ X_6]^T\ ,\ \ T_2 = [X_7\ X_8\ X_9]^T \qquad (12)$$

$$\text{Where } -16 \le X_i \le 16$$

III. Test System

A. IEEE 34-Bus Test System

IEEE 34-Bus Test System is an unbalanced radial system used for distributed generation. The single-line diagram of the system is given in Fig. 2.

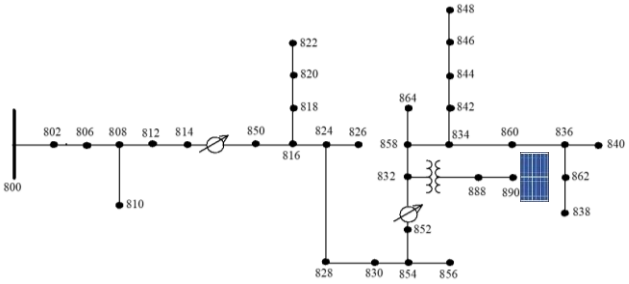

Fig. 2. The IEEE 34 Bus Test Feeder.

B. Load Profile

There are 3*33=99 prospective load buses in the system, where the first bus (grid connection point) is assumed to be load free. However, there are some loads that are distributed on some lines. Therefore, the number of load buses is (165) not 99 because the midpoint was added as a new bus during the simulation to account for the distributed loads. The nodes comprising the loads are given in Table 1.

TABLE I. DISTRIBUTION SYSTEM SPOT LOADS.

Node #	Active Power (kW)			Reactive Power (kVAr)		
	a	b	c	a	b	c
825	10	10	25	5	5	10
833	150	150	150	75	75	75
842	135	135	135	105	105	105
846	20	20	20	16	16	16
848	20	20	20	16	16	16
852	9	9	9	7	7	7

At this initial phase of the study, all the nodes are assumed to follow the same load pattern illustrated in Fig. 3. However, to account for the random behavior of the loads, a 5% random deviation from the recorded data is applied in each simulation time. That is, the load at any node at any time for any phase is randomly assigned a coefficient value between these limits.

C. Photovoltaic Unit

A 120 kW PV unit is installed at node 890 of the feeder as this node has the largest undervoltage. Daily active power generation data for a 15-minute time resolution is depicted in Fig. 4. On the other hand, the reactive power calculated by (11) is revised to satisfy a fixed power factor of 0.95 to represent the limit of a maximum reactive power that can be applied by the PV unit. This revised equation is presented in (13).

$$Q = \text{Min}\{\sqrt{S^2 - P^2}\ , P * \tan(\Phi)\ \} \qquad (13)$$

where $\Phi = \cos^{-1}(0.95)$ is the power factor, which is assumed to be over 0.95 in this study. The resulting reactive power capacity of the PV system is also illusrated in Fig. 4.

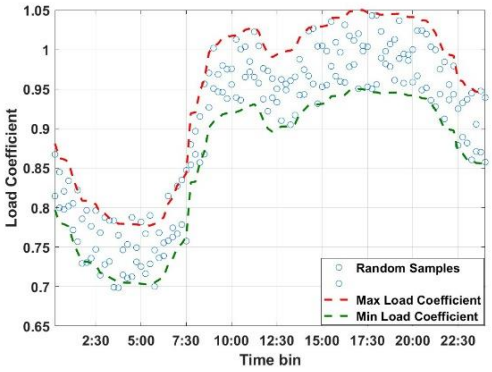

Fig. 3. Scaled load pattern for the distribution system.

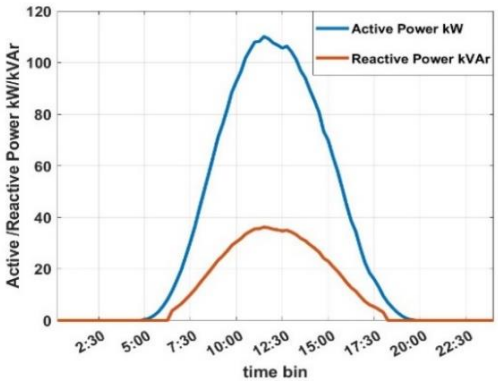

Fig. 4. PV output power for a constant power factor.

IV. Implementation of SQP Optimization

Sequential Quadratic Programming (SQP) is one of the powerful methods to solve constrained optimization problems. It linearizes the objective function quadratically and the constraints linearly and uses the exterior penalty function (EPF) to solve the linearized optimization problem. The proposed constrained nonlinear optimization problem formulated in (9) is solved by SQP method. The control variable vector comprises PV reactive power outputs and regulating transformers' tap ratios. Bus voltages are the state variables that are supposed to be within specified limits.

$$\boldsymbol{X} = [\mathbf{Q}^T\ \mathbf{T}_1^T\ \mathbf{T}_2^T]^T = [X_1\ X_1\ \ldots\ X_9]^T \qquad (14)$$

where $\boldsymbol{Q} = [X_1\ X_2\ X_3]^T$, $\boldsymbol{T}_1 = [X_4\ X_5\ X_6]^T$, $\boldsymbol{T}_2 = [X_7\ X_8\ X_9]^T$

$$\boldsymbol{V_{min}} \le \boldsymbol{V} = [V_1\ V_2\ \ldots.\ V_{165}]^T \le \boldsymbol{V_{max}} \qquad (15)$$

The solution steps of SQP implementation are as follows [22]:

- ***Step-1:*** Select an appropriate initial control variable, $\boldsymbol{X_0}$, and linearize the objective function around this point. The linearization is the quadratic expansion of the Taylor Series. The quadratic linearization of a function $F(X)$ around a point X_i can be expressed in (16) [22]:

$$F(X) = F(X_i) + \nabla F(X_i)^T X + \frac{1}{2} X^T \nabla^2 F(X_i) X \qquad (16)$$

where ∇, and ∇^2represent the gradient and the Hessian matrices, respectively.

- ***Step-2:*** Linearize the inequality constraints, G(X), around X_0 as shown in (17) [22].

$$G(X) = G(X_0) + \nabla G(X_0)^T \qquad (17)$$

- ***Step-3:*** Use Exterior Penalty Function (EPF) method to solve the linearized optimization problem in (18) [22]:

$$Minimize \quad F(x) + rg\ (max(0, G(X)))^2 \qquad (18)$$

where, rg is the penalty multiplier.

- ***Step-4:*** Update the operating point by adding the solution of the optimization problem in (18) as expressed in (19)[22].

$$X_{i+1} = X_i + X_{sol} \qquad (19)$$

where X_{sol} represents the solution vector of (18).

- ***Step-5:*** Check the convergence criteria and repeat the process from Step-1 if it is not met. The convergence criteria may be based on the change of the solution vector or the change of the objective function value as presented in (20) [22];

$$|X_{i+1} - X_i| \leq \in \text{ or } |F(X_{i+1}) - F(X_i)| \leq \in \qquad (20)$$

where $\in$ represents a small number, such 0.0001.

V. Simulation Results

SQP-based optimum solutions for the 34-bus test system are obtained separately for each 15-minute time bin throughout the day. The resulting control variables and corresponding voltage profiles are illustrated in the Figures (5-8) and Table. 2 below for some representative simulation periods.

A. Simulation at 10Δt (02:30 a.m.)

There is no active power generation and reactive power injection by PV unit at this time bin, and the only control parameters are the tap positions of the two regulating transformers. Optimal control parameters and corresponding voltage profiles are illustrated in Table 2 and Fig. 5, respectively. As it is an off-peak period, there are a few undervoltage violations around bus#96 for the base case operating conditions. All those violations are eliminated by optimizing the tap positions. However, some post-optimization voltage magnitudes approach their upper limits, especially for the buses after node 858.

B. Simulation at 35Δt (08:45)

The PV system can provide a limited amount of reactive power at 8:45 a.m. Optimal control parameters and their corresponding voltage profiles are illustrated in Table 2 and Fig. 6, respectively. For this case, all the undervoltage problems of the base-case operating conditions are eliminated with the help of optimized tap positions and limited reactive power injections of PV units. Note that the post-optimization voltage magnitudes of buses beyond 858 are now smaller than the previous case-A.

C. Simulation at 50Δt (12:30)

The reactive power injection potential of PV system is around its maximum, and the load is relatively high at this period. Optimal control parameters and corresponding voltage profiles are illustrated in Table 2 and Fig. 7, respectively. Note that the optimum voltage magnitudes are much closer to 1 pu. For this time bin.

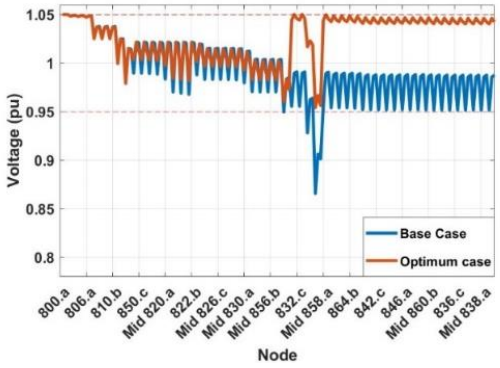

Fig. 5. Voltage Profiles at 02:30 a.m.

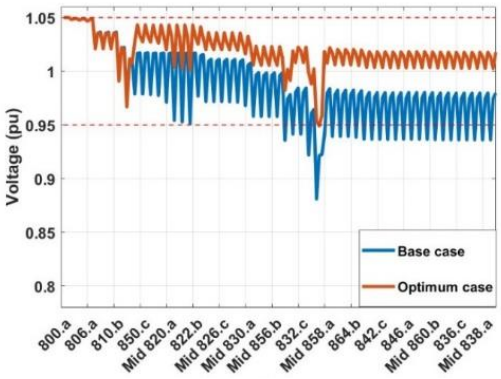

Fig. 6. Voltage Profiles at 08:45 a.m.

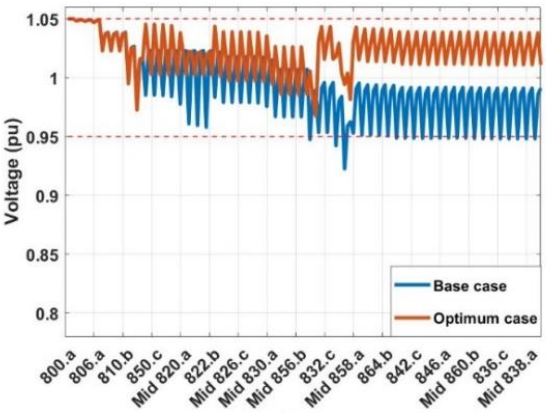

Fig. 7. Voltage Profiles at 12:30 p.m.

D. Simulation at 80Δt (20:00)

The load is maximum, but there is no PV active power generation and reactive power injection at 20:00. The optimal control parameters and corresponding voltage profiles are illustrated in Table 2 and Fig. 8, respectively. Due to the high load level, there are still undervoltage violations for few buses. Moreover, post-optimization voltage magnitudes of some buses are at their upper limit values.

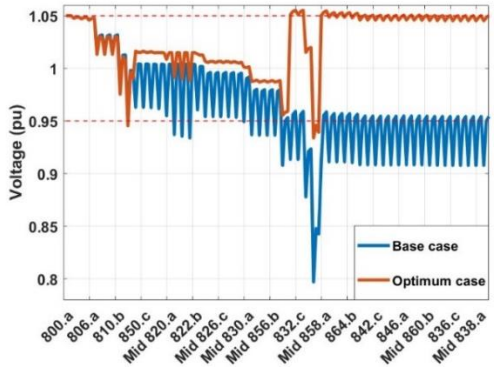

Fig. 8. Voltage Profile at 20:00 p.m.

TABLE II. OPTIMUM CONTROL PARAMETERS AND THEIR BASE-CASE VALUES

		Q [kVAr]			T_1			T_2		
Phase →		**a**	**b**	**c**	**a**	**b**	**c**	**a**	**b**	**c**
Base Case		0	0	0	1	1	1	1	1	1
Optimum	***At 02:30***	0	0	0	4	1	0	14	11	12
	At 08:45	-21	-21	-21	10	5	4	6	1	5
	At 12:30	-35	-28	-38	12	1	-2	4	10	8
	At 20:00	0	0	0	12	3	4	16	16	16

E. All day simulation

Optimum control parameters for all-day simulations are illustrated in Fig. 9. The voltage profiles for the base case and optimum operation cases are depicted in Fig. 10 and Fig. 11 for some representative buses, respectively. These buses are selected among the critical ones, either showing an undervoltage problem during the base case operating condition or an overvoltage for the optimum operating conditions.

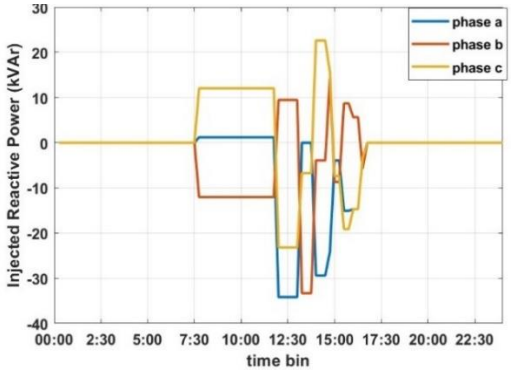

Fig. 9a. Injected reactive power from the PV unit throughout the day.

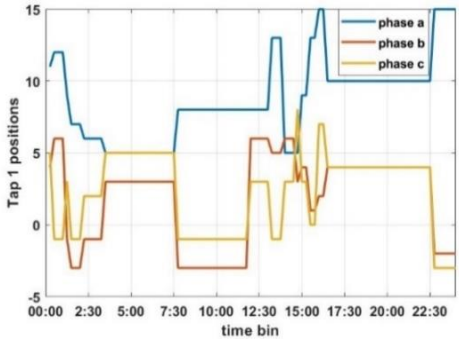

Fig. 9b. Tap 1 positions throughout the day.

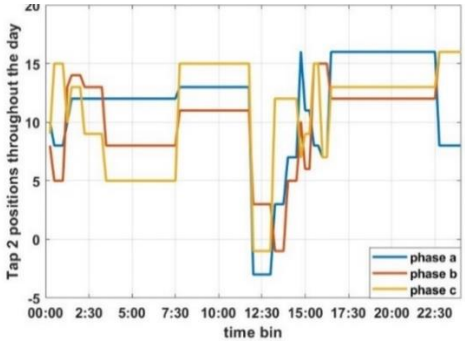

Fig. 9c. Tap 2 positions throughout the day.

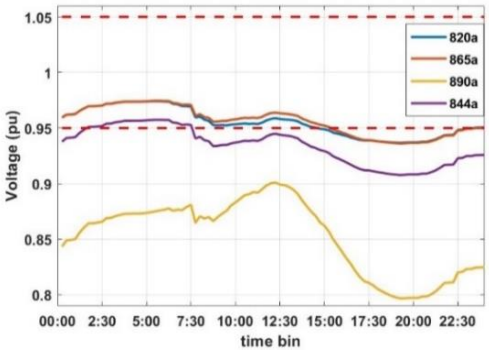

Fig. 10. Base case voltage magnitudes for some representative buses.

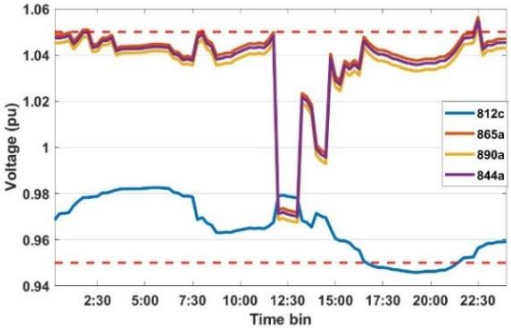

Fig. 11. Optimum voltage magnitudes for some representative buses.

VI. CONCLUSION

This study has presented SQP implementation to solve a nonlinear constrained optimization problem in a radial, unbalanced DN. The IEEE 34-bus test system is considered a test case for implementing the proposed method. The simulation

results for some representative times show that the performance of the voltage profile improvement objective depends on the available control variables and the load level. In this regard, we can decompose the day into three periods.

For the first period, where the load levels are low (late night-time –up to 9 a.m.), regulating transformers can regulate the voltage magnitude even without any contribution from the PV units. However, some bus voltage magnitudes approach their upper limits. Voltage magnitude differences get better after sunshine with the reactive power support of PV unit. The prospective problem of this region is the overvoltages and high losses due to insufficient reactive power support.

Both the load level and the PV output are high during the second period (9 a.m. to 5 p.m. for the given load and PV output characteristics). The voltage deviations and the losses are minimum in this period since the tap positions and reactive power injection of PV unit can actively be controlled.

The third region starts when the PV active power output decreases below 20% of the rated value (early evening, around 5 p.m.). Since the load level is relatively high in this region, there are severe undervoltages at base case operating conditions. Voltage regulators cannot eliminate all these undervoltage problems, instead, their high tap ratios force some feeder buses to operate at their upper voltage limits. In summary, there are both the undervoltage and overvoltage problems in this period. Therefore, power losses are maximum.

Since this method aims to improve the voltage profiles, the losses of the system can also be decreased. This will eventually reflect as a reduction in the electricity bill at the end of the month. The results can be used to improve active distribution management to deal with repeated operational actions.

ACKNOWLEDGMENT

This research is funded as a part of "120N996 Implementing digitalization to improve energy efficiency and renewable energy deployment in Turkish distribution networks" project under the framework of 2551 Project organized by TUBITAK and British Council.

REFERENCES

[1] J. A. P. Lopes, N. Hatziargyriou, J. Mutale, P. Djapic, and N. Jenkins, "Integrating distributed generation into electric power systems: A review of drivers, challenges and opportunities," Elect. Power Syst. Res., vol. 77, no. 9, pp. 1189–1203, 2007.

[2] Y. P. Agalgaonkar, B.C. Pal and R.A. Jabr, "Distribution Voltage Control Considering the Impact of PV Generation on Tap Changers and Autonomous Regulators," IEEE Trans. Power Syst., vol. 29, no. 1, pp. 182-192, Jan. 2014.

[3] Y. Zhu and K. Tomsovic, "Optimal Distribution Power Flow for Systems with Distributed Energy Resources," Int. J. Elect. Power Energy Syst., vol. 29, no. 3, pp. 260-267, Mar. 2007.

[4] Ahmadi, B., Ceylan, O., Ozdemir, A., "Grey wolf optimizer for allocation and sizing of distributed renewable generation", 54rd International Universities Power Engineering Conference, September 3-6 2019, Bucharest, Romania.

[5] Ahmadi, B., Ceylan, O., Ozdemir, A., "Distributed energy resource allocation using multi-objective grasshopper optimization algorithm," Electric Power Systems Research, Volume 201, Article Number107564, Dec. 2021.

[6] Ahmadi, B., Ceylan, O., Ozdemir, A., Fotuhi-Firuzabad, M., "A multi-objective framework for distributed energy resources planning and storage management," Applied Energy, 314(1):118887, May 2022.

[7] Ahmadi B, Ceylan O, Ozdemir A. A multi-objective optimization evaluation framework for integration of distributed energy resources. J Energy Storage 2021; 41:103005.

[8] S. Gill, I. Kockar and G.W. Ault, "Dynamic Optimal Power Flow for Active Distribution Networks," IEEE Trans. Power Syst., vol. 29, no. 1, pp. 121-131, Jan. 2014.

[9] Y. Zhu and K. Tomsovic, "Optimal Distribution Power Flow for Systems with Distributed Energy Resources," Int. J. Elect. Power Energy Syst., vol. 29, no. 3, pp. 260-267, Mar. 2007.

[10] N. Daratha, B. Das and J. Sharma, "Coordination Between OLTC and SVC for Voltage Regulation in Unbalanced Distribution System Distributed Generation," IEEE Trans. Power Syst., vol. 29, no. 1, pp. 289-299, Jan. 2014.

[11] M. J. Dolan, E. M. Davidson, I. Kockar,G.W. Ault and S. D. J. McArthur, "Distribution Power Flow Management Utilizing an Online Optimal Power Flow Technique," IEEE Trans. Power Syst. vol. 27, no. 2, pp. 790- 799, May 2012.

[12] S. Paudyal,C. A. Canizares and K. Bhattacharya, "Optimal Operation of Distribution Feeders in Smart Grids," IEEE Trans. Ind. Electron., vol. 58, no. 10, pp. 4495-4503, Oct. 2011.

[13] A. Borghetti, M. Bosetti, S. Grillo, S.Massucco, C. Nucci,M. Paolone,and F. Silvestro, "Short-term scheduling and control of active distribution systems with high penetration of renewable resources," IEEE Syst. J., vol. 4, no. 3, pp. 313–322, Sep. 2010.

[14] Q. Zhou and J.Bialek, "Generation curtailment to manage voltage constraints in distribution networks," IET Gener., Transm., Distrib., vol. 1, no. 3, pp. 492–498, May 2007.

[15] V. Calderaro, G. Conio, V. Galdi, G. Massa and A. Piccolo, "Optimal Decentralized Voltage Control for Distribution Systems with Inverter-Based Distributed Generators," IEEE Trans. Power Syst., vol. 29, no. 1, pp. 230-241, Jan. 2014.

[16] A. Borghetti, M. Bosetti, S. Grillo, M. Paolone, and F. Silvestro, "Short-Term Scheduling of Active Distribution Systems," in Proc. 2009 IEEE Power Tech Conf., Bucharest, Romania, Jun.28–Jul. 3 2009.

[17] A. Keane and M. O'Malley, "Optimal Allocation of Embedded Generation on Distribution Networks," IEEE Trans. Power Syst., vol. 20, no. 3, pp. 1640-1646, Aug. 2005.

[18] W. H. Kersting and D. L. Mendive, "An application of ladder network theory to the solution of three phase radial load flow problems", IEEE PES Winter Meeting, 1976.

[19] Jen-Hao Teng, "A direct approach for distribution system load flow solutions," in IEEE Transactions on Power Delivery, vol. 18, no. 3, pp. 882-887, July 2003.

[20] S. Elsaiah, M. Ben-Idris and J. Mitra, "Power flow analysis of radial and weakly meshed distribution networks," 2012 PES General Meeting, San Diego CA 2012, pp. 1-9

[21] Jen-Hao Teng, "A direct approach for distribution system load flow solutions," in IEEE Transactions on Power Delivery, vol. 18, no. 3, pp. 882-887, July 2003.

[22] Venkataraman, P., 2009. Applied Optimization with MATLAB Programming, second ed. John Wiley and Sons, Hoboken, NJ